Life time and mobility product of injected charge carriers in copper II phthalocyanine thin films with different phase structure

L. Enkhtur[a], R.Galbadrakh[a], G.Shilagardi[a], A. Babajanyan[b], K. Lee[b], D. Cha[b]

[a] *Department of Theoretical and Experimental Physics, National University of Mongolia , Ulaanbaatar, Mongolia*

[b] *Department of Physics and Interdisciplinary Program of Integrated Biotechnology, Sogang University, Seoul 121-742, Korea*

Using near-field scanning microwave microprobe (NSMM) method we have observed the distribution of injected charge carriers along conductivity channel in CuPc thin film on dependence of applied bias. From scan data were calculated diffusion length and product $\mu\cdot\tau$ for injected charges from Au electrode to CuPc thin film. By scanning electron microscopy method were investigated morphology properties of CuPc thin films, which explains the difference of product $\mu\cdot\tau$ for injected charge carriers in CuPc thin films with different crystal phase structure.

INTRODUCTION

The charge transport properties of conductivity channel of semiconductor thin films depend on distribution of injected charges. For the distribution of injected minority charges are important two meanings such as diffusion length and life time, which depend on recombination rate of charges. The diffusion length of injected minority carriers in inorganic semiconductors is well investigated by different methods [1-7]. The estimation of the minority carrier diffusion length by near-field photocurrent measurement of p-n junction in silicon using multi wavelength excitation gives values of 0.47 μm and 0.37μm for electrons and holes, respectively [1]. But the diffusion length of electrons in p-type silicon obtained by surface photovoltaic method is 45.52 μm [3]. Using electron beam induced current and current – voltage measurement was measured carrier diffusion length for electrons of (0.2±0.05) μm, which correspond to life time of 0.1 ns and diffusivity D_e of 2.6 cm^2s^{-1}[5]. Diffusion length measurements in p-HgCdTe using laser beam induced current gave value in range from 50 to 400 μm [6]. Also in [6] it is observed spatial distribution of excess electron concentration in device constructed on p-HgCdTe. By systematic investigation of minority carrier diffusion length in n- and p-GaN for nitride hetero junction bipolar transistor obtained that hole diffusion length is slightly decreased with increasing the doping concentration , and they were about 200 and 300 nm for the doping concentration of $5\cdot10^{17}$and $4\cdot10^{19}cm^{-3}$, respectively [7]. According [7], electrons diffusion length increased with decreasing the Mg doping concentration , and they were about 130 and 240 nm for doping concentration $4\cdot10^{18}$ and $9\cdot10^{19}$ cm^{-3} , respectively. Also it is shown that the minority electron diffusion length strongly depended on the dislocation density in the samples with doping concentration of $8\cdot10^{18}$ cm^{-3}.

Large spin diffusion length of 13.3 nm was measured in an amorphous organic semiconductor rubrene ($C_{42}H_{28}$) by spin polarized tunneling [8]. Injection of charge carriers into the LUMO and HOMO levels of CuPc is investigated by scanning tunneling microscopy [9]. Scanning gate microscopy of CuPc field effect transistors (FET) visualized the Shottky barriers at the metal/organic interfaces in real space [10]. Trapped carriers in polydiacetylene films were directly observed by the electric field induced second harmonic generation using FET structure [11]. Electric field distribution in channel of pentacene FET was successfully probed by microscopic optical second-harmonic generation (SHG) observation, and for FET at off state, enhanced SHG signal was observed, indicating the Laplace field formation reflecting the device geometry [12].

The computation of mobility lifetime product $\mu\cdot\tau$ takes into account the effects of the prevailing dangling occupation, and evaluated $\mu\cdot\tau$ product combines information about band mobility and defect density [13]. Also in Ref [13] established that $\mu\cdot\tau$ product is tool for correlating a-Si: H film properties and solar cell performances. In Ref [14] was investigated charge carrier mobility and lifetime versus composition of conjugated polymer/ fullerene bulk-heterojunction solar cells and revealed that the lifetime of the charge carriers decreases in such a way that the product $\mu\cdot\tau$ appears almost constant independently of the blend composition.

The surfaces of CuPc thin film, CuPC/ITO thin film and CuPC/ITO thin film on glass substrate were scanned by using NSMM method, and shown that the untensity variations

of the NFMM image are directly related to the changes of surface resistance of each thin films[15]. Earlier by NSMM imaging of pentacene FET was demonstrated the ability of this method to characterize the electric properties of thin films [16]. The modulation of electric potential properties along the FET channel by injection carriers was clearly observed by the NSMM method. In this paper by NSMM visualized distribution of injected charge from Au electrode to CuPc thin film deposited on glass substrate and after annealed at different temperatures.

MODELING OF MINORITY CARRIERS DRIFT IN AN ELECTRIC FILED

Let us now consider the diffusion of minority carriers on the semiconductor in external homogenous electric field according Ref [17]. Suppose, that there is $p-$type semiconductor ($p_0 \geq n_0$), which cross-section sizes much less than its length. Let we have two metallic contacts and in a zone of the negative contact ($-l \leq x \leq 0$) electrons are injecting to the semiconductor (Figure 1). A distance between contacts i.e. conductivity channel's length is L. Let concentration of the majority carriers p_0 is great in comparison with concentration of the minority carriers Δn, which has life time of τ_n. To the sample applied electric field ξ and carriers can drift in this electric field and diffuse into depth of the sample.

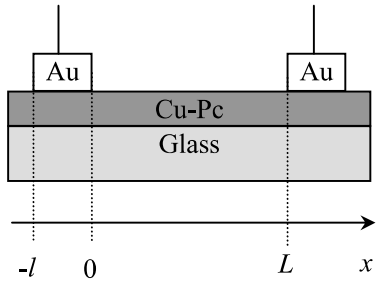

Figure 1. A scheme of organic semiconductor (Cu-Pc) thin film (on glass substrate) with metallic electrodes (Au).

The equation of continuity of electric current flow along x direction with the account of accumulation and generation of charges is

$$\frac{dn}{dt} = g + \frac{1}{e}\frac{\partial j_n}{\partial x} - \frac{\Delta n}{\tau_n}, \qquad (1)$$

Where g is the generation rate of electrons per volume 1 cm^3, j_n is current density due to electrons and

$$j_n = en\mu_n\xi + eD_n\frac{dn}{dx}\ . \qquad (2)$$

Where μ_n is mobility, D_n is diffusion coefficient of electrons. Substituting (2) to (1) in steady case ($\frac{dn}{dt} = 0$) yields

$$D_n\frac{d^2}{dx^2}\Delta n + \mu_n\xi\frac{d}{dx}\Delta n - \frac{\Delta n}{\tau_n} = 0. \qquad (3)$$

By dividing both parts of the equation on D_n and having following designations

$$L_D = \sqrt{D_n\tau_n}\,, \qquad (4)$$

$$L_\xi = \tau_n\mu_n\xi \qquad (5)$$

we will transform equation (3) to a kind

$$\frac{d^2}{dx^2}\Delta n + \frac{L_\xi}{L_D^2}\frac{d}{dx}\Delta n - \frac{\Delta n}{L_D^2} = 0. \qquad (6)$$

A common solution of last equation is

$$\Delta n = C_1e^{\alpha_1 x} + C_2e^{\alpha_2 x}. \qquad (7)$$

Where C_1 and C_2 are constant defined from boundary conditions, α_1 and α_1 are roots of characteristic equation

$$\alpha^2 + \frac{L_\xi}{L_D^2}\alpha - \frac{1}{L_D^2} = 0; \qquad (8)$$

$$\alpha_{1,2} = \frac{-L_\xi \pm \sqrt{L_\xi^2 + 4L_D^2}}{2L_D^2}. \qquad (9)$$

Considering the reduction of concentration of minority non equilibrium carriers in process of removal from contact, it is definitively received in case of $x \geq 0$

$$\Delta n = C_1e^{-\frac{x}{L_1}}, \qquad (10)$$

where

$$L_1 = \frac{2L_D^2}{\sqrt{L_\xi^2 + 4L_D^2} + L_\xi}. \qquad (11)$$

Also in case of $x \leq -l$

$$\Delta n = C_2e^{\frac{x}{L_2}}\,, \qquad (12)$$

where

$$L_2 = \frac{2L_D^2}{\sqrt{L_\xi^2 + 4L_D^2} - L_\xi}\,. \qquad (13)$$

Thus, in area on either side of contact the concentration of redundant minority carriers decreases on exponential law with decay constants L_1 and L_2. In absence of electric field, when $L_\xi = \tau_n\mu_n\xi = 0$, exists only the diffusion of redundant charge carriers. In this case redundant concentration of minority carriers

decreases by exponential decay on dependence of distance and characterized by value $L_D = \sqrt{D_n \tau_n}$, which is named diffusion length of redundant minority carriers. Consequently concentration of redundant minority carriers is changing on dependence of distance by law

$$\Delta n = \Delta n(0) e^{-\frac{x}{L_D}} \qquad (14)$$

When on the sample applied external electric field, the decay constants L_1 and L_2 are different from L_D. The values L_1 and L_2 named as 'diffusion length along field' and 'diffusion length against field' or 'length of tightening' [17].

SAMPLE PREPARATION

CuPc powder was purchased from Aldrich Chemical Co. and used without further purification. Slide glass was used as a substrate. The substrate was cleaned with acetone, ethyl alcohol and distilled water. The CuPc thin films are fabricated by the standard vacuum evaporation technique. A Cu-Pc source, contained in a ceramic crucible, was resistively heated in high vacuum chamber at 10^{-7} Torr. The deposition rate was controlled at 0.02 - 0.05 nm/sec. The resulting films were about 100 nm thick with deposition rate and thickness monitored by a thickness monitor. During deposition substrate temperature was 25 °C (room temperature). In order to study the effect of annealing three samples were prepared: as deposited thin film and films annealed at 200 °C and 350 °C for 1 hour. Gold contacts were deposited on the surface of the CuPc thin films with a thickness of 300 nm and a channel length of 50 μm.

EXPERIMENTAL SETUP

The optical absorption of the CuPc thin films was measured in the range 450-850 nm using a SCINCO UV-Vis spectrometer. The change of the crystal structure of CuPc thin films was inspected by x-ray diffraction. Surface morphology of the films was characterized by a scanning electron microscope (SEM). We have designed a NFMM system with a tuning fork distance control system to keep a constant distance between the sample and the tip. The probe tip was made of gold wire with a diameter of 50 μm with tapered end size of 1 μm. The probe tip was oriented perpendicular to the sample surface and the other end of the tip was directly connected to a coupling loop in the dielectric resonator. The reflection coefficient S_{11} was measured by network analyzer (Agilent 8722ES). To drive the tuning fork, an AC voltage was applied to one contact on the tuning fork at its resonance frequency using the oscillator of a lock-in amplifier. The resulting current from the other contact was measured by using the current input of the same lock-in amplifier. The output from the lock-in amplifier was fed into the feedback system to control the tip-sample distance using a piezo electric tube (PZT) that supports the sample stage. The probe tip to sample distance was kept at about 10 nm. All NSMM measurements were made at the same sample-tip distance. The sample was mounted onto an x-y-z-translation stage for coarse adjustment which was driven by a computer-controlled micro stepping motor with a resolution of 0.01 μm, whereas fine movement of the sample was controlled by a PZT tube.

RESULTS AND DISCUSSION

Figure 2 shows the optical absorption spectra of CuPc thin films deposited at room temperature and annealed at different temperatures for 1 hour. As shown in Figure 2, for the absorption spectra of the as-deposited thin film (RT) the higher energy maximum peak is larger than that of the second peak. Similar behavior is shown by the thin film annealed at 200 °C. This behavior represents the typical features of the α-phase of CuPc thin films. As the annealing temperature increased to 350 °C, the peak positions were changed to the maximum peaks positions of the β-phase of CuPc [18,19].

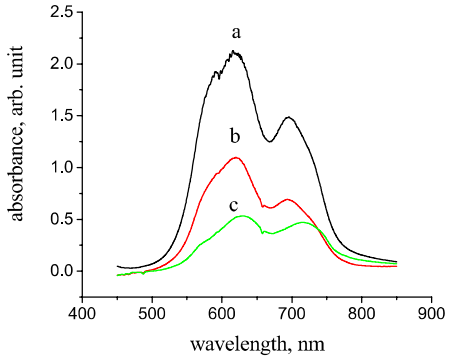

Figure 2. Optical absorption spectra of CuPc thin films : a- deposited at RT ; b- annealed at 200 ℃; c- annealed at 350 ℃.

Figure 3 shows the x-ray diffraction patterns for Cu-Pc thin films annealed at different temperatures. CuPc thin films deposited at room temperature showed only two distinct peaks at

6.7° and 13.5°, corresponding to the (002) and (400) lattice plane of the α-phase of CuPc. At the annealing temperature of 200 °C, five peaks corresponding to the crystal structure of the α-phase of CuPc were observed. CuPc thin films annealed at 350 °C showed the distinct eight peaks corresponding to the β-phase[20].

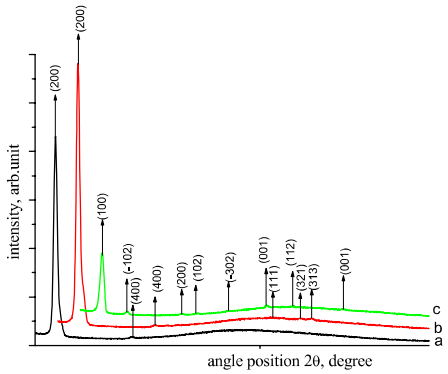

Figure 3. X-ray diffraction spectra of CuPc thin films : a- deposited at RT ; b- annealed at 200 ℃; c- annealed at 350 ℃.

From optical absorption spectra and X-ray data we conclude that CuPc thin films deposited at room temperature has semi disordered α-phase structure, but thin films after annealed at 200 °C and 350 °C have α- and β-phase structure.

To visualize the injected minority charge distribution in CuPc thin films under the external direct current biases we applied a near-field scanning microwave microprobe (NSMM) technique, which before us applied in Ref. [16]. We directly scanned the microwave reflection coefficient S_{11} of Cu-Pc thin film at 4.3 GHz. Figure 4 shows the line scanning results of CuPc thin films deposited at RT and annealed at 200 °C and 350 °C for 1 hour. The drain-source voltages were changed from 0 to 100 V by step of 10 V. Under set bias the line scanning correctly presents space distribution of injected carriers from Au electrode to CuPc thin film. Figure 4 shows, that the beginning of conducting channel pointed at position of 50 μm and channel end pointed at position 100 μm. Also shown, that the microwave reflection coefficient S_{11} is decreasing along channel, which significantly shows distribution of injected charges along the conductivity channel in CuPc thin film.

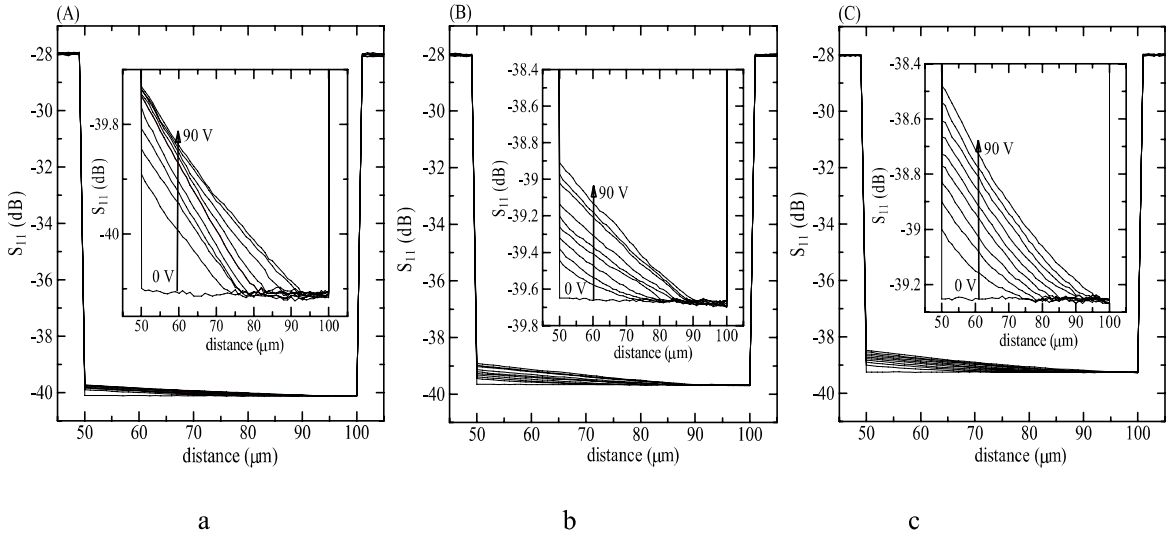

Figure 4. Line scans of Cu-Pc thin films: a- deposited at RT; b - annealed at 200 ℃; c- annealed at 350℃. Inset shows the magnified view of channel.

From scan results of CuPc thin films deposited at room temperature, annealed at 200° and 350° we defined length of tightening L_2 for each film on dependence of bias applied on electrodes (See Figure 4). Obtained experimental dependencies were fitted by function (17), where prior was substituted expression (8). Figure 5 shows fitted curves in comparison with experimental dependencies. By fitting procedure were revealed meanings of diffusion length L_D and product $\mu \cdot \tau$ of injected minority carriers for each investigated films, which are given in Table Obtained values of diffusion length are larger than results of [1] and [5] but less than that of [6] and [7]. The order of our values is comparable with spin diffusion length of 13.3 nm which measured in rubrene [8]. The values of obtained products $\mu \cdot \tau$ are comparable with that of a-Si:H

layers in annealed state above 160 °C [13]. Noticeable, calculation with using values of L_D and product $\mu \cdot \tau$ shows that Einstein relation is not valid for injected carriers from Au electrode to CuPc thin films.

Diffusion lengths of thin films deposited at RT and annealed at 200 °C after deposition close, but products $\mu \cdot \tau$ of them differ for 23 %. Diffusion length of Cu-Pc thin film annealed after deposition is less than that of other thin films. But products $\mu \cdot \tau$ of this film more that of thin films deposited at RT and annealed at 200 °C after deposition. The product $\mu \cdot \tau$ of thin film annealed at 200 °C after deposition has the least value. Ratio of product $\mu \times \tau$ of thin film deposited at RT and film annealed at 200 °C is 1.23, which we can compare with ratio $\mu_{||} / \mu_{\perp} = 1.4 \pm 0.1$, obtained from investigation of mobility anisotropies of Cu-Pc thin film field effect transistor [21]. Where $\mu_{||}$ is the mobility of charge carriers in case of current direction is along to longitude of domains of Cu-Pc thin film, and $\mu_{\perp}$ is the mobility of charge carriers when current direction perpendicularly to longitude of domains. Annealing at 350 °C for 1 hour increase product $\mu \cdot \tau$ of Cu-Pc thin film deposited at RT in 1.21 times. Difference of products $\mu \cdot \tau$ of investigated thin films we can explain by morphology of them.

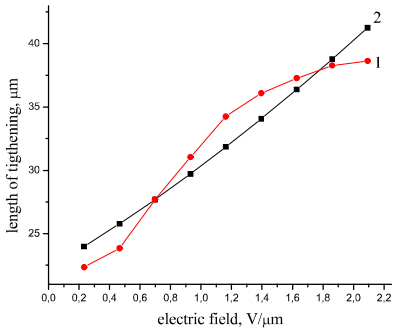

a

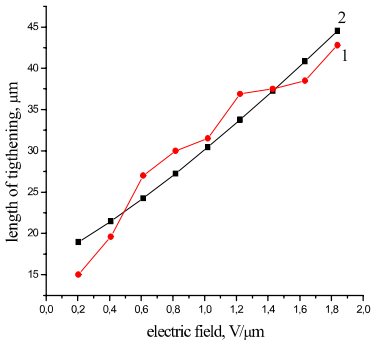

b

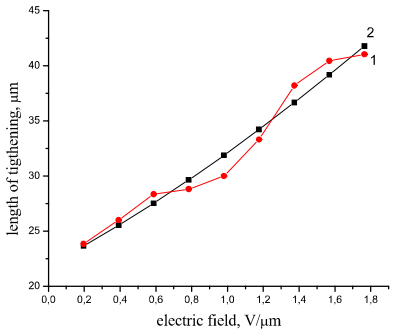

c

Figure 5. The tightening lengths dependence on applied electric field and fitted curves for CuPc thin films: a-deposited at RT; b-annealed at 200 °C; c-annealed at 350 °C. (1 - experimental dependence; 2 – fitted curve).

Table 1. Diffusion length and product $\mu \cdot \tau$ of Cu-Pc thin films.

CuPc thin film samples	Diffusion length L_D (μm)	Product μ·τ ($\mu m^2/V$)	Ratio of products μ·τ
Deposited at RT	21.90	17.17	$(\mu\cdot\tau)_{RT}/(\mu\cdot\tau)_{200°C}$= 1.23
Annealed at 200°	22.30	13.95	$(\mu\cdot\tau)_{350°C}/(\mu\cdot\tau)_{200°C}$=1.49
Annealed at 350°	16.70	20.84	$(\mu\cdot\tau)_{350°C}/(\mu\cdot\tau)_{RT}$= 1.21

SEM images of Cu-Pc thin films deposited at room temperature and annealed at 200°C and 350°C for 1 hour shown in Figure 6. In the scanning pattern of thin film deposited at room temperature were observed randomly located curved nanorods with are branching. Noticeable, nanorods are oriented along substrate. As result of the annealing at 200°C the morphology change and nanorods standing up perpendicularly to the

substrate surface, i.e. perpendicularly to direction of applied electric field. Meanwhile for thin film deposited at room temperature nanorods oriented along a direction of electric field applied on contacts. Consequently, according Ref. [21, 22], a mobility of thin film annealed at 200°C must lower that of thin film deposited at RT. The morphology of thin film annealed at 350°C is not homogenous and consist of different regions with various orientation of densely packed nanorods (Figure 6: c). Nanorods have lamellar like shape and the ends some of them like whiskers. In some regions elongated whiskers fell down and have horizontal position (Figure 6: d). The increasing of product $\mu\cdot\tau$ in result of annealing at 350°C we can explain, that during annealing process nanorods merged and the sizes have increased. According a reasoning of Ref. [21],the carrier mobility in a thin film FET is proportional to $l\exp(-E_b/kT)$, where l is semiconductor grain size and E_b is the energy for carrier detrapping from grain boundaries, when grains are large enough compared with Debye length L_D [23]. Rough estimation gives $L_D \sim 7$ nm for Cu-Pc, which is many times smaller than crystallite size.

Thus, we have established that product $\mu\cdot\tau$ for Cu-Pc thin films changes on dependence of annealing procedure, i.e. on dependence of morphology. Well known as annealing procedure changes crystal structure, morphology, carrier concentration, energy band gap of Cu-Pc thin film [21,25]. In our investigation changes of product $\mu\cdot\tau$ on dependence of annealing procedure we explain by anisotropic phenomenon and morphology of thin film.

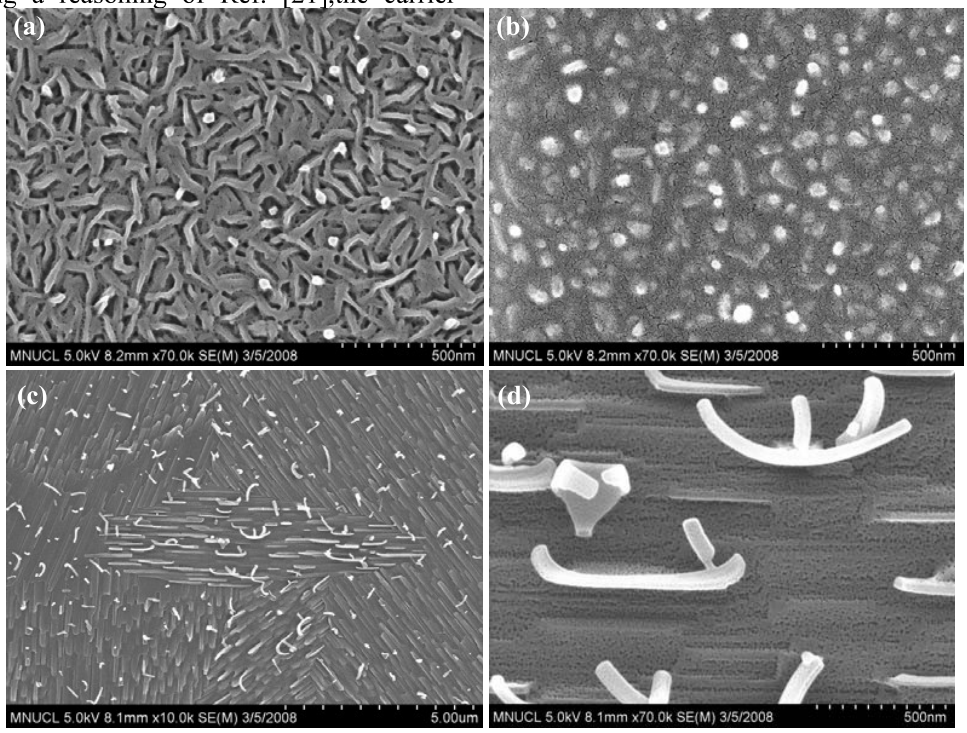

Figure 6. SEM images of CuPc thin films: a-deposited at RT; b-annealed at 200℃; c- annealed at 350℃; d – magnified part of the image of film annealed at 350℃.

CONCLUSION

By the NSMM method we revealed the space distribution of carriers injected from Au electrode to CuPc thin film. From scan data by calculated diffusion length and product $\mu\cdot\tau$ for CuPc thin film with different crystal phase structure. Value of product $\mu\cdot\tau$ of film deposited at RT higher in 1.23 times than that of film annealed at 200 ^{o}C, but for film annealed at 350 ^{o}C product $\mu\cdot\tau$ is higher than that for film deposited at RT. Changes of product $\mu\cdot\tau$ on dependence of annealing procedure we explain by anisotropic phenomenon and morphology of thin film. Investigation of morphology of CuPc thin films deposited on glass by scanning electron microscopy method revealed that in result of annealing at 200°C after deposition nanorods stand up perpendicularly to electric filed, while for thin film deposited at RT they are along the electric field direction. This phenomenon

explains decrease of product $\mu \cdot \tau$ on CuPc thin films annealed at 200°C.

Acknowledgments

This work was supported by Sogang University (2007), by Korean Foundation for Advanced Studies- International Scholar Exchange Fellowship for academic year 2007-2008, by the Korea Research Foundation (KRF-2005-042-C00058; KRF-2002-005-CS0003), Seoul Research and Business Development Program (10816) and by the Korea Science & Engineering Foundation (F01-2004-000-1082-0; R01-2006-000-11227-0), by projects H.1.7.2 and H.2.6.2 within the Innovation Development program of Mongolian Government.

Reference

[1]. [1] H. Fukuda, Y. Kadota and M.Ohstu. Jpn.J.Appl.Phys. 38 (1999) L571-L573.

[2]. [2] I.A.Bolesov, V.P.Karpov, and V.V.Karpov. Instruments and Experimental techniques, 46, No 2 (2003) 225-227.

[3]. [3] X.Zhang, G.He and J.Song. Semicond. and Sci. Technol. 7(1992) 888-891.

[4]. [4] A.Koo, F.Budde, B.J.Ruck, H.J.trodahl, A.Bittar, A.R.H.Peterson. J.Mater. Sci.: Mater. Electron (2007) 18:S107-S110.

[5]. [5] Z.Z. Bandic, P.M. Bridger, E.C. Piquette, and T.C. McGil . Appl. Phys. Let.73, n.22(1998)3276-3278.

[6]. [6] D.A.Redfern, J.A.Thomas, C.A.Musca, J.M.Dell, and L.Faraone Journal of Electronoic Materials, 30, No. 30 (2001), 696-703.

[7]. [7] K. Kumakura, T. Makimoto, N. Kobayashi, T. Hashizume, T. Fukui, and H.Hasegava. IEEE (2003) 49-50.

[8]. [8] J.H. Shim, K.V.Raman, Y.J. Park,T.S.Santos, G.X.Miao, B.Satpati, and J,S. Moodera. Phys. Rev. Let. PRL 100 (2008) 226603-1.

[9]. [9] S.F. Alvarado, L. Rossi, P. Muller, W. Rieb. Synthetic metals 122 (2001) 73-77.

[10]. [10] N. Aoki, K.Sudou, and K. Okamoto. Appl. Phys. Lett. 91(2007) 192113.

[11]. [11] T. Manaka, H. Kohn, Y. Ohshima, E. Lim, and M. Iwamoto. Appl. Phys. Lett. 90 (2007) 171119.

[12]. [12] T. Manaka, E. Lim, R. Tamura, D. Yamada, and M. Iwamoto. Appl. Phys. Lett. 89(2006) 072113.

[13]. [13] N. Beck, N. Wyrsch, Ch. Hof, and A. Shan.J.Appl. Phys. 79, No. 12 (1996) 9361

[14]. [14] G.Dennler, A.J. Mozer, G. Jucka, A. Pivrikas, R. Osterbacka, A. Fuchsbauer, N.S. Sariciftci. Organic Electronics 7(2006) 229-234.

[15]. [15] M. Park, H. Yoo, H.Yoo, S. Na, S.Kim, K.Lee, B. Friedman, E.Lim, M.Iwamoto. Thin Solid Films 499 (2006) 318-321.

[16]. [16] A.Babajanyan and K.Lee, E. Lim, T. Manaka and M.Iwamoto, B. Friedman. Appl. Phys. Lett. 90, 182104 (2007).

[17]. [17] K.V. Shalimova. Physics of semiconductors (in Russian), Energy, Mosow, 1971, pp. 202-207

[18]. [18 E. Jungyoon, S. Kim, E. Lim, K. Lee, D. Cha, B. Friedman, Appl. Surf. Sci. 205 (2003) 274.

[19]. [19] S. Karan, B. Malik, Solid State Commun. 143 (2007) 289.

[20]. [20] O. Berger, W. Fisher, B. Adolph, S. Tierbach, V. Melev, J. Sheirer, J. Mater. Sci. 11 (2000) 331.

[21]. [21] M. Ofuji, K. Ishikava, and H. Takezoe. Appl. Phys. Lett. 86 (2005) 062114.

[22]. [22] L. Chang, C. Wang, and M. Liu. Appl. Phys. Lett. 88 (2006) 202111.

[23]. [23] T.Yasuda, K. Fujita, H. Nakashima and T. Tsutsui. Jpn. Appl. Phys. 42 (2003) 6614-6618.